EXPLORING THE POSSIBLE ORIGINS OF MAGNETIZATION RECORDED IN APOLLO 11 MARE BASALTS. J. Jung[1] (jiinjung@stanford.edu), S. M. Tikoo[1,2], D. H. Burns[2], [1]Dept. of Geophysics, Stanford University, Stanford, CA 94305; [2]Dept. of Earth and Planetary Sciences, Stanford University, Stanford, CA 94305.

Introduction: The Moon does not generate a magnetic field today. However, numerous recent paleomagnetic studies on Apollo samples have shown that high surface magnetic field intensities (~40-110 μT) existed on the Moon between ~3.9 Ga and ~3.5 Ga (i.e., the high field epoch, or HFE) [1-4] (red circles in **Fig. 1**). Several large impact basins formed during and before this HFE period (e.g., Crisium, Nectaris) possess clear magnetic anomalies within their massive and slowly cooled (>10 kyr) central melt sheets, indicating that they acquired magnetization from a temporally stable dynamo field [5, 6].

Given the small lunar core size, however, the surface field strength of tens of μT cannot be explained by a continuously operating convective core dynamo [7]. Unconventional dynamo powering mechanisms have been suggested (e.g., a basal magma ocean dynamo [8], an impact-driven dynamo [5], mechanical dynamos driven by precession [9]), but none of these models can produce continuously strong surface fields during the HFE period (dash lines in **Fig. 1**).

Two explanations might resolve the mismatch between theoretical lunar dynamo models and the actual paleointensity results. First, the Moon may have experienced an intermittent (or episodically intense) dynamo [7, 10]. Many recent paleomagnetic studies specifically targeted high paleointensity samples from the Apollo-era dataset (1970 - 1980s). However, the Apollo-era measurements in aggregate show large paleointensity variability up to two orders of magnitude during the HFE [11-12] (gray circles in **Fig. 1**). This may be evidence for an episodically intense dynamo. However, we note that most of the Apollo-era paleointensity estimates need to be re-evaluated due to advances in methodology over time.

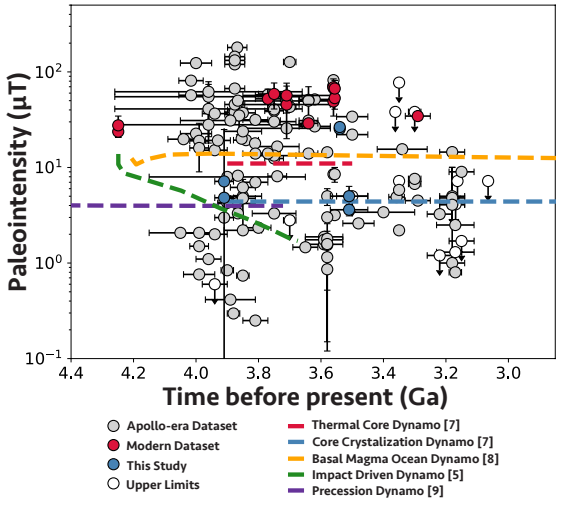

Fig. 1. Paleointensity determinations of apollo samples (circles) and estimated surface magnetic fields by theoretical dynamo models (dashed lines) vs age. Different datasets and models are colored differently. Ar-Ar radiometric age estimations are used to plot paleomagnetic datasets.

Second, lunar paleointensities may be affected by non-dynamo processes such as remagnetization by shock pressures [13], magnetization via transient impact-generated fields [14], acquisition of isothermal remanent magnetization (IRM) generated by spacecraft fields [15], or viscous remanent magnetization (VRM) after exposure to the geomagnetic field. Uncertainties may also result from samples' poor magnetic recording properties, methodological approaches, experimental settings, and acceptability criteria [15-17].

Here, we studied Apollo 11 mare basalts that formed with the goals of assessing paleointensity variability during the HFE and distinguishing between the aforementioned possible origins of magnetization.

Samples: Four HFE-aged mare basalts were analyzed. Two of them (e.g., 10003, 10069) were previously reported in the Apollo-era literature as having low paleointensity values (< 5 μT) [11, 18]. The other two (e.g., 10044, 10071) were previously unstudied. All samples were sliced into four mutually oriented sub-samples (~80 - 300 mg each).

Magnetic Carriers: Electron microprobe analyses and magnetic hysteresis parameters show that the predominant magnetic carriers are multidomain kamacite, although first-order reversal curve (FORC) diagrams hint at the existence of a higher coercivity (more single-domain-like) grain population. Except for sample 10044, no significant petrological evidence of shock features was observed (indicating peak pressures < 5 GPa) [19-20]. However, sample 10044 displayed undulatory extinction in pyroxene grains in sample 10044, indicating the sample experienced pressures > 5 GPa (**Fig. 2**).

NRM Behavior and Paleointensity: We conducted stepwise alternating field (AF) demagnetization and non-heating anhysteretic remanent magnetization (ARM) paleointensity experiments on three sub-samples from each rock ("a-c") (**Fig. 2**). Each "a" piece was subjected to an additional IRM paleointensity experiment (IRM of 0.9 T). We used calibration factors of f' = 1.30 and a = 2070 μT for the ARM and IRM methods, recalculated from the supplementary table from [3]. All sub-samples had very low coercivity (LC1: 0-5 mT), low coercivity (LC2: 2-13 mT), and medium coercivity (MC: 9-50 mT) overprints. VRM and long-

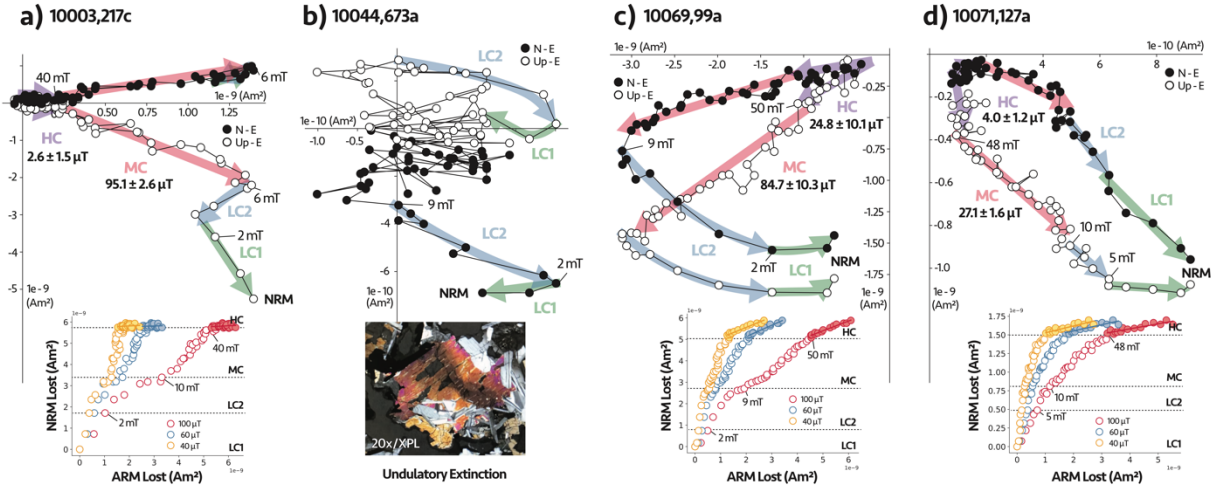

Fig. 2. Zjiderveld plots for subsamples from 10003 (a), 10044 (b), 10069 (c), 10071 (d). Colored shadings represent different magnetization components. Insets of (a), (c), and (d) show ARM paleointensity experimental results (ARM lost vs NRM lost) with different ARM dc-bias fields. Mean paleointensities for each component are labeled on the Zijderveld diagrams. Inset of (b) shows an optical photograph of sample 10044 showing an undulatory extinction of pyroxene grains.

term IRM acquisition experiments [15] suggest that these overprints were likely acquired via exposure to the Earth's magnetic field and/or fields generated from the Apollo spacecraft. The behavior of high coercivity (HC) components (30-100 mT) of each sample are described below:

***10003*:** Principal component analyses (PCA) of subsamples indicate that HC components have a high maximum angular deviation (MAD) of ~40-45°. The ARM and IRM paleointensity estimations are 4.83 ± 6.53 μT and 7.15 ± 17.80 μT, respectively.

***10044*:** Sample 10044 was not a good target sample to retrieve a reliable paleointensity. HC components show non-origin trending, unstable demagnetization patterns.

***10069*:** HC components were stable and unidirectional across subsamples. These components are origin-trending (MAD > deviation angle (DANG)), which might indicate a primary thermal remanent magnetization (TRM) origin. The calculated ARM and IRM paleointensities are 24.93 ± 0.90 μT and 26.49 ± 1.94 μT, respectively. These are ~10x larger than reported values in Apollo-era literature for the same sample [11, 18].

***10071*:** HC components of 10071 are unidirectional across mutually oriented subsamples and are origin-trending (MAD > DANG), though MAD ranges from ~38-45°. 10071 has a very weak paleointensity of 3.98 ± 0.74 μT (ARM) and 5.01 ± 1.33 μT (IRM).

Discussion: Our results show diverse paleointensity estimates from HFE-aged Apollo 11 mare basalt samples (blue circles in **Fig. 1**). Sample 10044 may have lost its original magnetic record due to shock demagnetization by impact events. We obtained ~25 μT paleointensity values for sample 10069, which are similar to other modern paleointensity estimates of HFE mare basalts. However, with the same non-heating paleointensity methods, we also obtained potentially null and very low paleointensity values from 10003 and 10071, respectively. Our results may indicate magnetic fluctuations during the HFE corresponding to an intermittent dynamo [7, 10] or dynamo processes analogous to the Earth, including magnetic reversals or excursions [21]. Ongoing work will assess potential contributions from non-dynamo field sources.

Acknowledgments: We thank R. Ziegler and J. Gross, CAPTEM, and the Lunar Receiving Laboratory at Johnson Space Center for allocating and preparing our samples. We also thank the Institute of Rock Magnetism (IRM) at the University of Minnesota, especially P. Solheid, for assistance with hysteresis and FORC measurements. This research was supported by a NASA FINESST award number 80NSSC21K1541.

References: [1] Shea E. K., et al. (2012) *Sci., 335,* 453-456. [2] Suavet C., et al. (2013) *PNAS, 110*, 8453-8458. [3] Weiss B. P. and Tikoo S. M. (2014) *Sci., 346,* 1246753. [4] Nichols C. I. O., et al., (2021) *Nat. Ast., 5,* 1216-1223. [5] Le Bars M., et al., (2011) *Nat., 479,* 215-218. [6] Tsunakawa H. F., et al., (2015) *JGR. Planets*, *120*, 1160-1185. [7] Evans A. J., et al., (2018) *GRL, 45*, 98-107. [8] Scheinberg A. L., et al., (2018) *EPSL*, *492*, 144-151. [9] Dwyer C. A., et al., (2011) *Nat, 479,* 212-214 [10] Evans A. J. and Tikoo S. M., (2022), *Nat. Ast.,* 6, 325-330. [11] Cisowski S. M., et al. (1983) *LPSC*, *88*, A691-A704. [12] Fuller M. and Cisowski S. M. (1987) *Geomagnetism, 2,* 307-455. [13] Jung, J., et al., (2021) *LPSC LII*, 2388. [14] Tarduno J. A., et al., (2021) *Sci. Adv., 7,* eabi7647. [15] Tikoo S. M., and J. Jung., (2023) *LPSC LIV*, submitted. [16] Lawrence K., et al., (2008) *Phys. Earth Planet. Inter., 168*, 71-87. [17] Tikoo S. M., et al., (2012) *EPSL, 332-338*, 93-103. [18] Helsey C. E., (1970) *GCA. Suppl. 1,* 2213. [19] Stöffler D. G., et al. (2006) *Rev. Mineral. Geochem. 60,* 519-596. [20] Fritz J. A., et al., (2017) *Meteorit. Plant. Sci. 52,* 1216-1232. [21] Selkin P. A. and Tauxe L. (2000) *Phios. T. R. Soc. A., 258*, 1065-1088.